

A Particle-Filtering Based Approach for Distributed Fault Diagnosis of Large-Scale Interconnected Nonlinear Systems

Elaheh Noursadeghi, Ioannis Raptis

Mechanical Engineering Department, University of Massachusetts Lowell

Email: {Elaheh_Noursadeghi, Ioannis_Raptis}@uml.edu

Abstract—This paper deals with the problem of designing a distributed fault detection and isolation algorithm for nonlinear large-scale systems that are subjected to multiple fault modes. To solve this problem, a network of detection nodes is deployed to monitor the monolithic system. Each node consists of an estimator with partial observation of the system's state. The local estimator executes a distributed variation of the particle filtering algorithm; that process the local sensor measurements and the fault progression model of the system. In addition, each node communicates with its neighbors by sharing pre-processed information. The communication topology is defined using graph theoretic tools. The information fusion between the neighboring nodes is performed by a distributed average consensus algorithm to ensure the agreement on the value of the local estimates. The simulation results demonstrate the efficiency of the proposed approach.

Index Terms—distributed fault diagnosis, large-scale systems, particle filtering, networked control systems, sensor networks, information fusion.

I. INTRODUCTION

The majority of the systems that are frequently encountered in all aspects of our everyday life; describing technological, environmental, financial and social processes are characterized by considerable size and significant complexity. In the technical world, contemporary industrial processes are composed by a large number of spatially distributed feedback modules with heterogeneous sensors, actuators and controllers that exchange information over a band-limited communication network that is embedded to the system. These systems are characterized as large-scale networked control systems and can be found in many real-life applications such as: telecommunication networks, water distribution systems, traffic networks, power systems, multi-vehicle formations to name a few.

Every system is susceptible to faults that may lead to catastrophic failures. Complex processes are significantly more vulnerable to faults, since a malfunction in a single component may have a major effect to the entire system. There is a growing need for reliable real-time monitoring and supervision especially in the case of safety-critical systems. The broad objective is to design fault tolerant systems that maintain their operation even in the occurrence of faults. A timely diagnosis of a fault mode may improve the system's availability and maintainability by avoiding down-times, breakdowns and catastrophic failures.

Fault diagnosis has received considerable attention since the 1970s. Most of the existing techniques involve a centralized architecture [1]–[6], where a single diagnostic module is responsible of receiving, and processing all the information measured by the sensors. This architecture is appropriate for small and centralized systems, however, it is ill-suited for large-scale systems with spatially distributed components. Every monitoring system has certain limitations in terms of computational power and communication bandwidth. When the dimensionality and complexity of the system increases, it is likely that these limitations will not be satisfied by a centralized configuration.

It is of great importance to express the formulation of fault diagnosis in a non-centralized way, making it applicable to real-life large-scale systems [7]–[12]. Existing methodologies interchange different types of data between their detecting nodes such as: state estimates [7], [11], [13], raw measurements of the interconnected states [8]–[10], or fault signatures [11]. The first distributed fault diagnosis approach using particle filtering was introduced in [14], [15]. In general, the majority of the existing distributed techniques are designed for discrete-event systems [16]–[18].

In this work, we present a full-order Distributed Particle Filtering Fault Diagnosis (DPFFD) algorithm for large-scale nonlinear/non-Gaussian systems. The design objective is to develop a network of interconnected Detector Nodes (DNs) to monitor a stochastic nonlinear process that is subject to a set of active fault modes. The DNs should detect distributively the occurrence of a fault by computing the probability of failure of each mode. Each DN has access to a partial and noisy measurement of the system's state and to processed statistical information from its neighboring nodes. It consists of an embedded processing unit that computes a local PF algorithm and a consensus filter that fuses the processed information of neighboring DNs such that the entire detecting system reaches an agreement of its estimates. Graph-based abstractions will be used to represent the active communication channels between the nodes. The output of the detection network is a filtered estimate of the process state and a probability of failure for each fault mode.

The paper is organized as follows: A brief description of the centralized particle filtering algorithm is presented in Section II. A centralized particle filtering fault diagnosis approach is analytically introduced in Section III. In Section

represents the dynamic of fault mode j . The term $\beta(k - k_0)$ is a scalar function representing the time profile of the fault occurrence that takes place at some unknown time k_0 . Here, we can consider both types of faults: *abrupt* (step-like) or *incipient* (exponential-like) faults, described by:

$$\beta(k - k_0) = \begin{cases} 0 & k < k_0 \\ \underbrace{1}_{\text{abrupt}} \text{ or } \underbrace{1 - c^{-(k-k_0)}, c > 1}_{\text{incipient}} & k \geq k_0 \end{cases} \quad (6)$$

The algorithm incorporates the process model of (5), as well as a binary state vector, to detect changes in the process dynamics expressed by the terms $\beta(k - k_0)$. To this end, a vector of binary states $b^j(k) = [b_1^j(k) \ b_2^j(k)]^T$ with $b_1, b_2 \in [0 \ 1]$ and $j = 1, \dots, M$, is used to signal the occurrence of each fault mode. More specifically, $b_1^j(k) = 1$ indicates that the system is operating normally, while $b_2^j(k) = 1$ denotes the presence of fault mode j in the system. This technique enables us to calculate probabilistic measures related to the existence of a fault in the system.

To determine the operating condition of the system (normal or faulty operating condition) and make a decision based on occurrence of faults, a particle filtering approach will be employed for a statistical characterization of both the binary and continuous-valued states, as new measurements are received. The binary states update sequence is augmented to the state-transition model S given in (7). This way, the state-transition model of system S is converted to a *failure sensitive filter* that reflects the presence of changes to the original healthy dynamics. Hence, the state vector that is used by the PF algorithm is $\mathcal{X}^T(k) = [(x^c(k))^T \ (b^1(k))^T \ \dots \ (b^M(k))^T] \in \mathbb{R}^{n_x+2 \cdot M}$, where $x^c(k) = x(k)$. The state-space model of the system that is implemented in the PF algorithm can be expressed in terms of the continuous states vector, and the binary states vector. Therefore, the state-transition model of these two state vectors and the measurement equation can be written as:

$$\begin{aligned} x^c(k+1) &= f(x^c(k), u(k)) + \sum_{j=1}^M g^j(x^c(k), u(k)) \cdot b_2^j(k) \\ &\quad + \tilde{v}(k) \\ b^j(k+1) &= \Phi(b^j(k) + n^j(k)) \quad j = 1, \dots, M \\ z(k+1) &= h(x^c(k)) + \tilde{\omega}(k) \end{aligned} \quad (7)$$

where $\tilde{v}(k)$, and $\tilde{\omega}(k)$ are the approximations of non-Gaussian process and measurement noise with appropriate dimensions, respectively. These noise sequences should be as close as possible to the actual ones ($v(k)$ and $\omega(k)$). The evolution of the binary states $\Phi: \mathbb{R}^2 \rightarrow \{[0 \ 1]^T, [1 \ 0]^T\}$, is a nonlinear function driven by the identically independent distributed (i.i.d) uniform white noise $n^j(k)$. The function $\Phi(\cdot)$ is defined such that the previous state $b^j(k)$ is randomly excited at each time step by $n(k)$. This random vector of \mathbb{R}^2 is assigned to ones of the binary states (healthy/faulty) based on the distance metric of the perturbed vector $b^j(k) + n(k)$ to the coordinates $[0 \ 1]^T$ and $[1 \ 0]^T$. With this technique, when a fault occurs, the weights will gradually converge the binary state $b_2^j(k)$ to

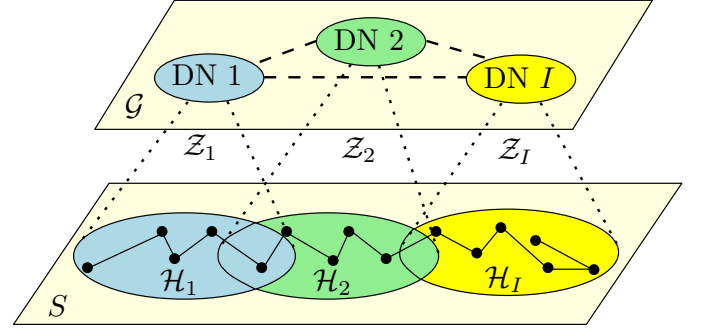


Figure 2. Block diagram of DPFFD approach

one ($b_2^j(k) \rightarrow 1$). This is due to the fact that the likelihood of the measurements will diminish the weights of particles associated with the healthy condition. A choice of $\Phi(\cdot)$ that has been successfully used in [20]–[23] is:

$$\Phi(x) = \begin{cases} e_1 & \text{if } \|x - e_1\| \leq \|x - e_2\| \\ e_2 & \text{else} \end{cases} \quad (8)$$

where $e_1 = [1 \ 0]^T$ and $e_2 = [0 \ 1]^T$. The state model of the CPFFD algorithm can be written in a more compact form as:

$$\begin{aligned} \mathcal{X}(k+1) &= \mathcal{F}(\mathcal{X}(k), u(k), \mathcal{V}(k)) \\ \mathcal{Z}(k) &= \mathcal{H}(\mathcal{X}(k)) + \tilde{\omega}(k) \end{aligned} \quad (9)$$

where $\mathcal{V} = [v^T(n^1)^T \dots (n^M)^T]^T$, $\mathcal{Z} = z$, and $\mathcal{F}(\cdot)$, $\mathcal{H}(\cdot)$ are nonlinear functions of appropriate dimensions and structure calculating based on (7). The above definition will be used to ease the notation in the subsequent parts of this paper. The outputs of the CPFFD module are the *probabilities of each failure mode*. These are the expectations of the binary states $\hat{b}_2^j(k) = E[b_2^j(k) | z(k)]$. This value is used to trigger alarm indicators if its value exceeds a certain threshold $\alpha \in (0 \ 1)$ that marks the probability of detection (i.e. $\hat{b}_2^j(k) < \alpha$ indicates normal operation). With this layout two or more different co-existing fault modes can be simultaneously detected.

IV. DISTRIBUTED PARTICLE FILTERING FAULT DIAGNOSIS

The CPFFD algorithm described in the previous Section is not scalable or robust for complex large-scale dynamical systems that employ scattered measurement sensors over large geographical regions.

Here, we propose a Distributed Particle Filtering Fault Diagnosis (DPFFD) algorithm for large-scale nonlinear/non-Gaussian systems. The main objective is to develop a network of interconnected Detector Nodes (DNs) to monitor the full-order system that is subject to a set of active fault modes. Figure 2 indicates the block diagram of the proposed distributed approach. Similar to Section II, we assume the presence of M potential fault modes in system S (5). A network of N DNs is deployed to monitor the full-order system. The local measurement equation of each of which is expressed by:

$$z_I(k) = h_I(x(k)) + \omega_I(k) \quad I = 1, 2, \dots, N \quad (10)$$

where $z_I(k) \in \mathbb{R}^{n_{z_I}}$ refers to the observation vector of DN I ; the nonlinear function $h_I : \mathbb{R}^{n_x} \rightarrow \mathbb{R}^{n_{z_I}}$ indicates the local measurement dynamics, and ω_I stands for its corresponding measurement noise.

Analogously to (9), a compact formulation of the state-transition model that is used by the local PF module at each DN can be written as:

$$\begin{aligned} \mathcal{X}(k+1) &= \mathcal{F}(\mathcal{X}(k), u(k), \mathcal{V}(k)) \\ \mathcal{Z}_I(k) &= \mathcal{H}_I(\mathcal{X}(k)) + \hat{\omega}_I(k) \end{aligned} \quad (11)$$

where $\mathcal{Z}_I = z_I$; $\mathcal{F}(\cdot)$ is calculated according to (7), and $\mathcal{H}_I(\cdot)$ is a nonlinear function that represents the local measurement dynamic (10). It is reminded that \mathcal{X} includes both the continuous system's states vector $x^c = x$ as well as the binary states vector $b^j(k) = [b_1^j(k) \ b_2^j(k)]^T$, $j = 1, \dots, M$.

As mentioned, the goal of the DPFFD algorithm is to estimate the full system's state $\mathcal{X}(k)$ in a sequential manner and diagnose distributively the occurrence of the fault modes based on the local measurement vector of each DN.

Graph-based abstractions will be used to represent the active communication channels between the nodes. The communication network will be described by the graph \mathcal{G} , defined as the pair $\mathcal{G} = (\mathcal{V}, \mathcal{E})$, where $\mathcal{V} = \{v_1, \dots, v_N\}$ is the vertex set or DNs set, and $\mathcal{E} = \{\{v_i, v_j\} \in \mathcal{V} \times \mathcal{V}\}$ represents the set of edges of \mathcal{G} . Each element of \mathcal{E} represents an undirected communication link between two DNs. The neighborhood $\mathcal{N}_i \subseteq \mathcal{V}$ of the vertex v_i is defined as the set of all vertices that are adjacent to v_i , $\{v_j \in \mathcal{V} | \{v_i, v_j\} \in \mathcal{E}\}$. If $v_j \in \mathcal{N}_i$, it follows that $v_i \in \mathcal{N}_j$, since an undirected edge exists between them.

The algorithm is performed in several steps at each DN in parallel with other neighboring nodes. Each DN executes a local bootstrap PF (*particle update*). In the first step, N_s particles are drawn according to the state transition equation of (11).

The next step is the *weight update step*. In this step, each node uses its local observation and communicates with its neighbors to update its particle weights based on $p(\mathcal{Z}(k) | \mathcal{X}^i(k))$. The main problem here is that each DN does not have access to global observation vector (it is defined as the union of local observation vectors, $\mathcal{Z}(k) = \bigcup_{I=1}^N \mathcal{Z}_I(k)$). To calculate the value of $p(\mathcal{Z}(k) | \mathcal{X}^i(k))$ in a distributed manner at each DN, each node requires to calculate its local likelihood function $p(\mathcal{Z}_I(k) | \mathcal{X}^i(k))$ based on its observation and communicates with its neighboring nodes.

To calculate the value of $p(\mathcal{Z}(k) | \mathcal{X}^i(k))$ in a distributed manner, we assume that the local measurement noise sequences of the DNs are independent. Therefore, the global likelihood function can be factorized as the product of the local likelihood distributions [24]–[26] as:

$$p(\mathcal{Z}(k) | \mathcal{X}(k)) = \prod_{I=1}^N p(\mathcal{Z}_I(k) | \mathcal{X}(k)) \quad (12)$$

The above equation requires the same set of particles $\{\mathcal{X}_I^i(k)\}_{i=1}^{N_s} = \{\mathcal{X}^i(k)\}_{i=1}^{N_s}$, $I = 1, \dots, N$ is sampled at each iteration, hence, the synchronization of the local random number generators of DNs is necessary. The synchronous

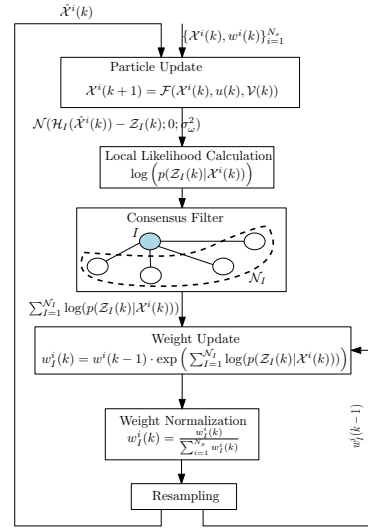


Figure 3. Schematic of the DPFFD algorithm's execution flow in DN I .

operation of the DNs can be achieved by use of random number generators with identical seeds that are initialized at the same points. Therefore, each DN calculates its local likelihood function based on its observation vector. Following (4) and the factorization of the global likelihood distribution given in (12), the particle weights are calculated as follows:

$$w_I^i(k) = w^i(k-1) \cdot \left(\prod_{J \in \{I, \mathcal{N}_I\}} p(\mathcal{Z}_J(k) | \mathcal{X}^i(k)) \right) \quad (13)$$

where $\prod_{J \in \{I, \mathcal{N}_I\}} p(\mathcal{Z}_J(k) | \mathcal{X}^i(k))$ indicates the product of the local likelihood functions of node I and its neighboring nodes represented by \mathcal{N}_I . Since, it is often easier to work with the logarithm of a probability rather than the probability itself, we take the natural logarithm from (13). Therefore, applying the natural logarithm [24] yields to:

$$\log \left(\prod_{I=1}^N p(\mathcal{Z}_I(k) | \mathcal{X}^i(k)) \right) = \sum_{I=1}^N \log p(\mathcal{Z}_I(k) | \mathcal{X}^i(k)) \quad (14)$$

The above sum can be calculated in a distributed way by means of distributed average consensus algorithm [27], [28] and communication graph topology. The consensus filter is executed iteratively in every time step of the DPFFD algorithm. The input of the consensus filter at each DN is the logarithm of the local likelihood function, $\log p(\mathcal{Z}_I(k) | \mathcal{X}^i(k))$. In the consensus algorithm, each DN computes $\sigma_I = \sum_{J \in \{I, \mathcal{N}_I\}} \left(\log p(\mathcal{Z}_J(k) | \mathcal{X}^i(k)) \right)$ iteratively by communicating with its neighbors across the pre-defined graph topology and use of the weighted average as:

$$\sigma_I(t+1) = \mathcal{W}_{II} \sigma_I(t) + \sum_{J \in \mathcal{N}_I} \mathcal{W}_{IJ} \sigma_J(t) \quad I = 1, \dots, N \quad (15)$$

where \mathcal{W}_{II} and \mathcal{W}_{IJ} are fixed weights. We employ the Metropolis weights to calculate the value of \mathcal{W}_{IJ} [27], [28].

Note that the time index of the consensus filter is denoted by t indicating that the algorithm is iterated at every time step k of the local PF algorithm. The algorithm is executed until

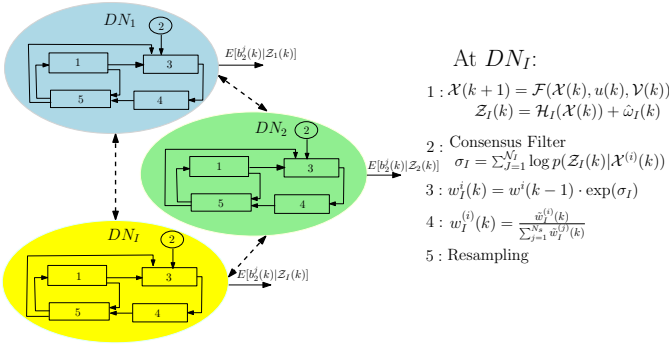


Figure 4. Block diagram of the DPFFD algorithm.

a certain convergence error is achieved or a pre-determined number of iterations is reached. In fact, the consensus filter plays the role of observation fusion center. Its output relies on two factors: i) type of the consensus algorithm; and ii) the communication graph topology between DNs. Finally the particle weights are updated according to:

$$w_I^i(k) = w^i(k-1) \cdot \exp \left(\sum_{J \in \{I, \mathcal{N}_I\}} \log p(\mathcal{Z}_J(k) | \mathcal{X}^i(k)) \right) \quad (16)$$

The schematic of the local PF algorithm performed in one of the DNs is depicted in Figure 3. Other steps include: weight normalization, resampling, and MMSE state estimate performed in the same way as explained in Section II.

The output of each DN is the probabilities of the failure modes $\hat{b}_2^j(k) = E[b_2^j(k) | \mathcal{Z}_I(k)]$. It is important to note that due to the consensus filter embedded at each DN, we have $E[b_2^j(k) | \mathcal{Z}_I(k)] = E[b_2^j(k) | \mathcal{Z}(k)]$. This equality states that the probability of each failure mode has the same value in every DN due to the execution of the distributed agreement protocol. Similar to the centralized case, this value is used to trigger alarm indicators if it exceeds a certain threshold $\alpha \in (0, 1)$ that marks the probability of detection. The block diagram of the DPFFD algorithm is depicted in Figure 2. During the execution of the diagnostic routine, each DN computes its local likelihood function based on a reduced-order measurement of the system's state. Then, each DN broadcasts its local processed data to the consensus filter that is used to compute the particle weights. An illustration of the full-order DPFFD algorithm is depicted in Figure 4. The pseudo code is provided in Table I.

V. NUMERICAL RESULTS

The DPFFD algorithm was evaluated via numerical simulations. The system under investigation is a chemical process consisted of nine identical interconnected tanks filled with a liquid. The cross section of the cylindrical tanks and their connection are denoted by S_c and S_p , respectively. The tanks are arranged in a grid formation as shown in Figure 5. The level of tank i is denoted by x_i and is determined by means of the mass balance equations as:

$$\dot{x}_i = \frac{1}{S_c} \left(\sum Q_{j,i} - \sum Q_{i,k} \right) + v_i \quad (17)$$

Table I
DPFFD ALGORITHM.

```

1: for  $I = 1 : N$  do
  Initialization:
2:    $\mathcal{X}^T(0) = [ \underbrace{1 \ 0}_{\text{mode 1}} \dots \underbrace{1 \ 0}_{\text{mode j}} \dots \underbrace{1 \ 0}_{\text{mode M}} \ x_c^T(0) ]$ 
3:   At time  $k \geq 1$ 
  Particle Update:
4:    $\mathcal{X}(k+1) = \mathcal{F}(\mathcal{X}(k), u(k), \mathcal{V}(k))$ 
  Weight Update:
5:    $w_I(k) = w(k-1) \cdot \prod_{I=1}^N p(\mathcal{Z}_I(k) | \mathcal{X}^i(k))$ 
6:    $\log \left( \prod_{I=1}^N p(\mathcal{Z}_I(k) | \mathcal{X}^i(k)) \right) =$ 
7:      $\underbrace{\exp \left( \sum_{I=1}^N \log p(\mathcal{Z}_I(k) | \mathcal{X}^i(k)) \right)}_{\text{distributed average consensus}}$ 
  Weight Normalization:
8:    $w_I^i(k) = \frac{w_I^i(k)}{\sum_{i=1}^{N_s} w_I^i(k)}$ 
  Resampling
  Calculation of MMSE state estimate:
9:    $\hat{\mathcal{X}}(k) = \sum_{i=1}^{N_s} w_I^i(k) \mathcal{X}^i(k)$ 
  Calculation the probability of each failure mode:
10:  for  $j = 1 : M$  do
11:     $E[b_2^j(k) | \mathcal{Z}(k)] = \frac{\sum_{i=1}^{\text{number of particles with } b_2^j(k)=1} w_I^i(k)}{\sum_{j=1}^{N_s} w_I^j(k)}$ 
12:  end for
13: end for

```

Table II
MODEL PARAMETERS OF THE WATER TANK SYSTEM

Parameter	Meaning	Value
$x_i(0)$	Initial level of tanks	$2m$
S_p	Cross section of interacting pipes	$2 \times 10^{-5} m^2$
S_c	Tank cross sectional area	$0.0154 m^2$
μ_i	Flow correction term	1
g	Gravity constant	$9.81 \frac{m}{s^2}$

where $Q_{j,i}$ represents the flow rate from tank j to tank i (inflow rate to tank i), and $Q_{i,k}$ refers to the flow rate from tank i to tank k (outflow rate from tank i), and v_i stands for the process noise. The flow rate variable, $Q_{i,j}$, is defined by means of Torricelli's rule as:

$$Q_{i,j} = \mu_i \cdot S_p \cdot \text{sign}(x_i - x_j) \cdot \sqrt{2g|x_i - x_j|} \quad (18)$$

where the nominal values of the parameters in (17) and (18) is given in Table II.

The three fault modes under consideration are leakages to tanks 4, 5 and 7 (The fault modes are depicted with double arrows in Figure 5). The leakage model at tank i is described by:

$$g^i(x_i) = \left(\frac{\mu_i \cdot S_p}{S_c} \right) \text{sign}(x_i) \sqrt{2g|x_i|} \quad (19)$$

To apply the DPFFD approach, we discretize the system with a sampling period of $T_s = 0.1 s$. The monolithic system is monitored by three DNs (dashed lines in Figure 5). We define a *full-connectivity graph topology* among the DNs. The state transition and the observation model of the DNs are expressed

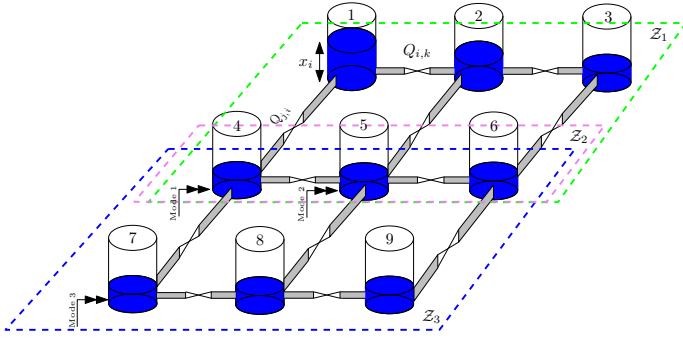


Figure 5. Schematic of the nine-tank system monitored by three DNs. The location of the fault nodes is highlighted by the double arrows.

as:

$$\begin{aligned}
 x &= [x_1 \dots x_9]^T \\
 x_J(k+1) &= f(x_J(k)) + v_J(k) \quad J = \{1, \dots, 9\} \\
 x_I(k+1) &= f(x_I(k)) + \sum_{j=1}^3 b_{2,I}^j \cdot \left(\frac{\mu_I \cdot S_p}{S_c} \right) \text{sign}(x_I) \sqrt{2g|x_I|} \\
 &\quad + v_I(k) \quad I = 4, 5, 7 \\
 z_1(k) &= \mathcal{I}_6 \times [x_1, \dots, x_6]^T + \omega_1(k) \\
 z_2(k) &= \mathcal{I}_3 \times [x_4, \dots, x_6]^T + \omega_2(k) \\
 z_3(k) &= \mathcal{I}_6 \times [x_4, \dots, x_9]^T + \omega_3(k)
 \end{aligned} \tag{20}$$

where $v_J(k)$ is selected as normal distribution, $\mathcal{N}(0, 0.05)$, and $\omega_I(k)$ $I = 1, \dots, 3$ is chosen as multivariate normal distribution, $\mathcal{N}(0_{n_{z_I}}, \Sigma)$ with covariance matrix $\Sigma = a \times \mathcal{I}_{n_{z_I}}$ and $\mathcal{I}_{n_{z_I}} \in \mathbb{R}^{n_{z_I} \times n_{z_I}}$ denotes the identity matrix. The positive constant $a = 0.2$ is selected 10% of the nominal value of the tank's level. The binary state vector b_I^j is stimulated by the binary noise in the range $[-0.75 \ 0.75]$. The probability of each fault mode and the estimation results of the DPFFD algorithm are depicted in Figures 6 and 7, respectively. The results are the same for all three DNs. Figure 6 shows the probability of the different failure modes occurring in the system and calculated by the DNs. As it can be seen from this figure, all three DNs can diagnose the fault modes 1, 2, and 3 at time instances $T = 200, 250, 290$ s as expected. The comparison of the real value via the estimated value of the level of the tanks is illustrated in Figures 7 and 8, respectively. Figure 8 indicates the actual and the estimated value corresponding to tank 4. The simulation results were deemed satisfactory. The DNs accurately and timely identified all fault modes filtered the system's state.

VI. CONCLUSION

This paper presents a distributed diagnostic module, suitable for large-scale and spatially distributed nonlinear stochastic systems. Instead of a central diagnostic unit, the system is monitored by a set of interconnected detection nodes with local processing and communication capabilities. Graph theoretic tools are deployed to represent the communication topology of the system. Every node executes a consensus protocol that steers the output of the entire network to a common estimate.

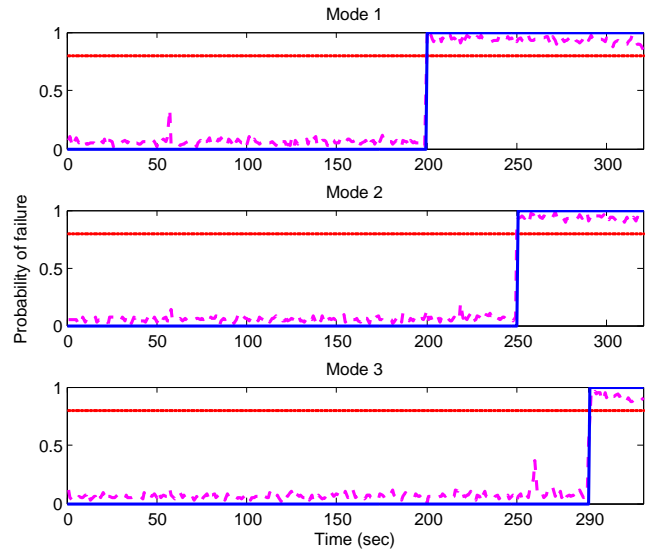


Figure 6. Probability of failure for each fault mode calculated by the DNs (dashed magenta line), failure mode occurrence (solid blue line), and threshold level (solid red line).

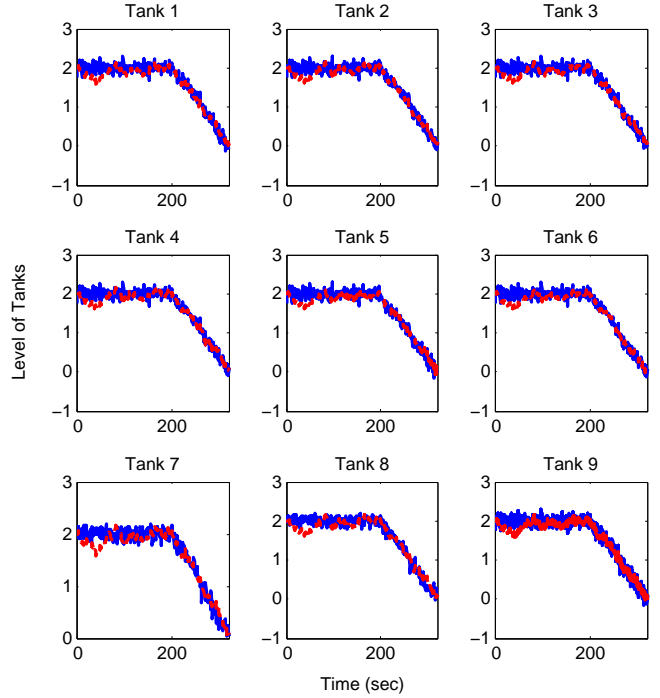


Figure 7. Comparison of the actual (solid blue line) and estimated value (dashed red line) of the liquid level with respect to time

REFERENCES

- [1] Kabore, P., and Wang, H., 2001. "Design of fault diagnosis filters and fault-tolerant control for a class of nonlinear systems". *Automatic Control, IEEE Transactions on*, **46**(11), pp. 1805–1810.
- [2] Zhang, X., Polycarpou, M., and Parisini, T., 2001. "Robust fault isolation for a class of non-linear input-output systems". *International Journal of Control*, **74**(13), pp. 1295–1310.
- [3] Jiang, B., Staroswiecki, M., and Cocquempot, V., 2004. "Fault diagnosis based on adaptive observer for a class of non-linear systems with unknown parameters". *International Journal of Control*, **77**(4), pp. 367–383.

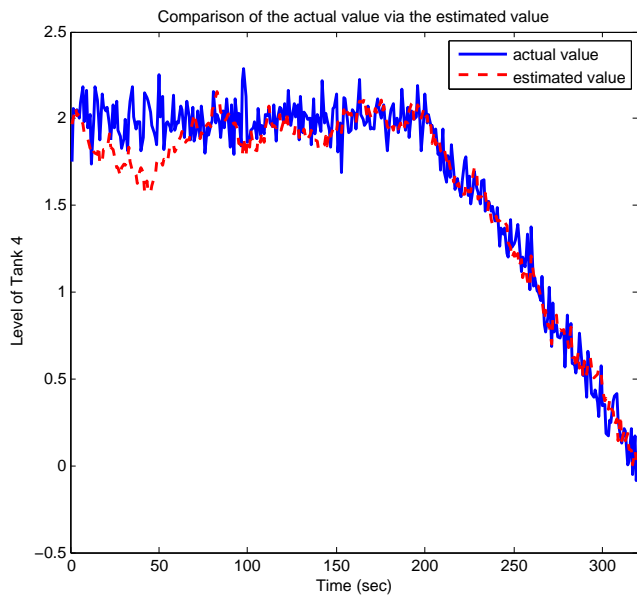


Figure 8. Comparison of the actual vs the estimated value of the liquid level in tank 4.

- [4] Xu, A., and Zhang, Q., 2004. "Nonlinear system fault diagnosis based on adaptive estimation". *Automatica*, **40**(7), pp. 1181–1193.
- [5] Chen, W., and Saif, M., 2007. "A sliding mode observer-based strategy for fault detection, isolation, and estimation in a class of lipschitz nonlinear systems". *International Journal of Systems Science*, **38**(12), pp. 943–955.
- [6] Tang, X., Tao, G., and Joshi, S. M., 2007. "Adaptive actuator failure compensation for nonlinear mimo systems with an aircraft control application". *Automatica*, **43**(11), pp. 1869–1883.
- [7] Zhang, X., and Zhang, Q., 2012. "Distributed fault diagnosis in a class of interconnected nonlinear uncertain systems". *International Journal of Control*, **85**(11), pp. 1644–1662.
- [8] Ferrari, R. M. G., Parisini, T., and Polycarpou, M. M., 2012. "Distributed fault detection and isolation of large-scale discrete-time nonlinear systems: An adaptive approximation approach". *IEEE Transactions on Automatic Control*, **57**(2), pp. 275–290.
- [9] Boem, F., Ferrari, R. M., Parisini, T., and Polycarpou, M. M., 2013. "Distributed fault diagnosis for continuous-time nonlinear systems: The input-output case". *Annual Reviews in Control*, **37**(1), pp. 163–169.
- [10] Shames, I., Teixeira, A. M., Sandberg, H., and Johansson, K. H., 2011. "Distributed fault detection for interconnected second-order systems". *Automatica*, **47**(12), pp. 2757–2764.
- [11] Daigle, M. J., Koutsoukos, X. D., and Biswas, G., 2007. "Distributed diagnosis in formations of mobile robots". *IEEE Transactions on Robotics*, **23**(2), pp. 353–369.
- [12] Davoodi, M. R., Khorasani, K., Talebi, H. A., and Momeni, H. R., 2014. "Distributed fault detection and isolation filter design for a network of heterogeneous multiagent systems". *IEEE Transactions on Control Systems Technology*, **22**(3), pp. 1061–1069.
- [13] Yan, X.-G., and Edwards, C., 2008. "Robust decentralized actuator fault detection and estimation for large-scale systems using a sliding mode observer". *International Journal of control*, **81**(4), pp. 591–606.
- [14] Cheng, Q., Varshney, P. K., Michels, J., and Belcastro, C. M., 2005. "Distributed fault detection via particle filtering and decision fusion". In 8th International Conference on Information Fusion, Vol. 2, IEEE, pp. 8–pp.
- [15] Cheng, Q., Varshney, P. K., Michels, J. H., and Belcastro, C. M., 2009. "Distributed fault detection with correlated decision fusion". *Aerospace and Electronic Systems, IEEE Transactions on*, **45**(4), pp. 1448–1465.
- [16] Baroni, P., Lamperti, G., Pogliano, P., and Zanella, M., 1999. "Diagnosis of large active systems". *Artificial Intelligence*, **110**(1), pp. 135–183.
- [17] Rish, I., Brodie, M., Ma, S., Odintsova, N., Beygelzimer, A., Grabarnik, G., and Hernandez, K., 2005. "Adaptive diagnosis in distributed systems". *IEEE Transactions on Neural Networks*, **16**(5), pp. 1088–1109.
- [18] Le, T., and Hadjicostis, C. N., 2006. "Graphical inference methods for fault diagnosis based on information from unreliable sensors". In 9th International Conference on Control, Automation, Robotics and Vision (ICARCV), IEEE, pp. 1–6.
- [19] Ristic, B., Arulampalam, S., and Gordon, N., 2004. *Beyond the Kalman filter: Particle filters for tracking applications*. Artech house.
- [20] Orchard, M. E., 2007. "A particle filtering-based framework for on-line fault diagnosis and failure prognosis".
- [21] Orchard, M. E., and Vachtsevanos, G. J., 2009. "A particle-filtering approach for on-line fault diagnosis and failure prognosis". *Transactions of the Institute of Measurement and Control*, **31**(3-4), pp. 221–246.
- [22] Raptis, I. A., and Vachtsevanos, G., 2011. "An adaptive particle filtering-based framework for real-time fault diagnosis and failure prognosis of environmental control systems". *Proceedings of the Prognostics and Health Management*.
- [23] Raptis, I. A., Sconyers, C., Martin, R., Mah, R., Oza, N., Mavris, D., and Vachtsevanos, G. J., 2013. "A particle filtering-based framework for real-time fault diagnosis of autonomous vehicles". In Annual Conference of the Prognostics and Health Management Society.
- [24] Hlinka, O., Hlawatsch, F., and Djuric, P. M., 2013. "Distributed particle filtering in agent networks: A survey, classification, and comparison". *IEEE Signal Processing Magazine*, **30**(1), pp. 61–81.
- [25] Coates, M., 2004. "Distributed particle filters for sensor networks". In Proceedings of the 3rd international symposium on Information processing in sensor networks, ACM, pp. 99–107.
- [26] Sheng, X., and Hu, Y.-H., 2005. "Distributed particle filters for wireless sensor network target tracking". In IEEE International Conference on Acoustics, Speech, and Signal Processing (ICASSP), Vol. 4, pp. iv–845.
- [27] Xiao, L., and Boyd, S., 2004. "Fast linear iterations for distributed averaging". *Systems & Control Letters*, **53**(1), pp. 65–78.
- [28] Xiao, L., Boyd, S., and Lall, S., 2005. "A scheme for robust distributed sensor fusion based on average consensus". In Fourth International Symposium on Information Processing in Sensor Networks, pp. 63–70.